

Spin-dependent dynamically assisted Schwinger mechanism

Xu-Guang Huang^{1,2} and Hidetoshi Taya^{1,*}

¹*Department of Physics and Center for Field Theory and Particle Physics, Fudan University, Shanghai, 200433, China*

²*Key Laboratory of Nuclear Physics and Ion-beam Application (MOE), Fudan University, Shanghai 200433, China*

(Dated: June 13, 2022)

We study electron and positron pair production from the vacuum by a strong slow electric field superimposed by a weak fast electric field as a perturbation (the dynamically assisted Schwinger mechanism). We argue that the Schwinger mechanism becomes spin-dependent if the perturbation has a transverse component with respect to the strong electric field. We analytically/numerically compute the difference between the production number of spin up and down particles. We find that the spin-imbalance is strongly suppressed by an exponential of the critical field strength if the frequency of the perturbation is small, while it is only weakly suppressed by powers of the critical field strength if the frequency is large enough. We also find that the spin-imbalance exhibits non-trivial oscillating behaviors in terms of the frequency of the perturbation, the azimuthal angle, and the transverse momentum of produced particles.

I. INTRODUCTION

The spontaneous electron and positron pair production from the vacuum in the presence of classical electric field (the Schwinger mechanism) is one of the most remarkable predictions of quantum electrodynamics (QED) [1–3]. Intuitively, the physical origin of the Schwinger mechanism is essentially the same as the electrical breakdown of semi-conductors (or the Landau-Zener transition [4–7]). That is, the energy band of electrons is tilted by the electric field, so that electrons filling the Dirac sea can tunnel into the positive energy band leaving holes in the Dirac sea (i.e., positrons). The tunneling rate should be suppressed exponentially by the tunneling length, i.e., the gap energy $\sim 2m$. Therefore, one expects that the Schwinger mechanism can be manifest only when the typical energy scale of the electric field becomes larger than the gap energy. Indeed, the production number for a constant and homogeneous electric field was explicitly computed by Schwinger in his seminal work in 1951 [3] as

$$n_{\mathbf{p},s}^{(\mp)} = \frac{V}{(2\pi)^3} \exp \left[-\pi \frac{m^2 + \mathbf{p}_\perp^2}{eE} \right], \quad (1)$$

where $n^{(-/+)}$ is for electrons/positrons. This formula implies that one has to prepare an extremely strong electric field of the order of $eE_{\text{cr}} \equiv m^2 \sim \sqrt{10^{28}} \text{ W/cm}^2$ to test the Schwinger mechanism in laboratory experiments. Unfortunately, it seems to be impossible to achieve this within current experimental technologies. Indeed, HERCULES is the present strongest laser, whose strength is $eE \sim \sqrt{10^{22}} \text{ W/cm}^2$ [8]. There are many intense laser facilities planned around the world (e.g. ELI [9], HiPER [10]), which are expected to reach $eE \sim \sqrt{10^{24}} \text{ W/cm}^2$ but are still weaker than the critical field strength E_{cr} by several orders of magnitude.

Recently, there has been an increasing interest in how to enhance the production number of the Schwinger mechanism. One of the most reasonable ideas is to superimpose a weak fast electromagnetic field onto the original electric field (the dynamically assisted Schwinger mechanism) [11–15]. This idea can be understood as an analog of the Franz-Keldysh effect in semi-conductor physics [16–20]. An intuitive explanation of the idea is the following: Firstly, the weak fast field perturbatively interacts with electrons in the Dirac sea to kick them up into the gap. Then, the tunneling length for the Schwinger mechanism is reduced by the kick, so that the critical field strength E_{cr} is effectively reduced as the frequency of the weak fast field is increased. Notice that the perturbative kick is the essence for the dynamically assisted Schwinger mechanism. This point was clarified in Refs. [20–22] by explicitly employing a perturbation theory in terms of the weak field in the Furry picture [20–25]. In particular, it was shown that the production process is dominated by the perturbative kick for a weak field with frequency above the gap energy. In that limit, the production number becomes proportional to powers of eE/m^2 , which is free from the strong exponential suppression.

In this paper, we discuss a novel effect due to the superposition of a weak fast electric field in the Schwinger mechanism. Namely, we show that the Schwinger mechanism becomes spin-dependent if the superimposed electric field is transverse with respect to the original strong electric field. Notice that the original Schwinger mechanism (1) is clearly spin-independent because the quantum tunneling is insensitive to spin. The superimposition of an additional transverse electric field is essential for the spin-dependence. Intuitively, this is because a particle with transverse momentum feels a magnetic field in the longitudinal direction in its rest frame if the superimposed electric field in the observer frame has transverse component with respect to the momentum direction. Therefore, the mass gap is effectively reduced/enhanced through the spin-magnetic coupling depending on the charge and the momentum direction, which results in the spin-dependent Schwinger mechanism. Note that a sim-

* h_taya@fudan.edu.cn

ilar spin-dependent particle production mechanism from the vacuum was recently studied in Ref. [26], in which the electron-positron pair production by a rotating electric field in the multi-photon production regime was considered.

This paper is organized as follows: In Sec. II, we analytically study the aforementioned spin-dependent Schwinger mechanism with superposition of a weak fast field based on a perturbation theory in the Furry picture [20–25]. In Sec. III, we numerically solve the Dirac equation to discuss the spin-dependent Schwinger mechanism without relying on any approximations. The numerical results are compared with the analytical formula obtained in Sec. II, and we find an excellent agreement between them. Section IV is devoted to summary and discussion. Details of the analytical calculations in Sec. II are presented in Appendix A.

II. ANALYTICAL DISCUSSION BASED ON PERTURBATION THEORY IN THE FURRY PICTURE

In this section, we analytically show that the Schwinger mechanism becomes spin-dependent if one superimposes a weak electric field: We first explain our physical setup in Sec. II A. Nextly, in Sec. II B, we derive a formula for the momentum distribution of electrons and positrons produced by the Schwinger mechanism with a weak fast field by employing a perturbation theory in the Furry picture [20–25]. By using this formula, we compute the difference between the production number of spin up and down particles in Sec. II C. We show that the difference becomes non-vanishing if the weak field is transverse, and discuss its qualitative features.

A. Setup

We consider QED in the presence of external classical field A_μ , whose Lagrangian is given by

$$\mathcal{L} = \bar{\psi} [i\cancel{\partial} - e\cancel{A} - m] \psi. \quad (2)$$

In this work, we assume that the external field is purely electric and homogeneous in space. We also adopt the temporal gauge $A_0 = 0$, so that A_μ depends only on time $A_\mu(x) = A_\mu(x^0)$ in the following.

We consider a situation in which A_μ can be separated into two parts, i.e., strong slow field \bar{A}_μ and weak fast perturbation on top of it \mathcal{A}_μ as

$$A_\mu = \bar{A}_\mu + \mathcal{A}_\mu. \quad (3)$$

We also assume that the strong field \bar{A}_μ is sufficiently slow, so that it can be approximated by a constant electric field as

$$\bar{A}_\mu = (0, 0, 0, \bar{E}x^0), \quad (4)$$

where $e\bar{E} > 0$ and we defined the x^3 -axis by the direction of the strong electric field. Furthermore, we in this work focus on the simplest perturbation, i.e., a monochromatic electric wave with frequency $\Omega > 0$,

$$\mathcal{A}_\mu = \sin(\Omega t + \phi) \times (0, a_1, a_2, a_3), \quad (5)$$

where ϕ is an arbitrary phase factor. It is straightforward to generalize the following discussions to other types of perturbations. Note that the electric field strength \mathcal{E} for this perturbation reads $|\mathcal{E}| \sim |\mathbf{a}|\Omega$, so that the Keldysh parameter [27–30] is given by $\gamma_K \equiv m\Omega/|\mathcal{E}| = m/|\mathbf{a}|$. This implies that the effect of the perturbation remains “perturbative” and the perturbation theory in the Furry picture becomes valid if $|\mathbf{a}| \lesssim m$ is satisfied. Otherwise $|\mathbf{a}| \gtrsim m$, higher order corrections due to multiple scatterings with the perturbation contribute to the production process non-perturbatively, which is difficult to discuss within the perturbation theory in the Furry picture¹. We also note that the dynamically assisted Schwinger mechanism with a similar but different weak field configuration (i.e., on-shell dynamical photon) $\mathcal{A}_\mu \propto \sin(\Omega(t - \mathbf{n} \cdot \mathbf{x}) + \phi)$ with \mathbf{n} being a unit vector $|\mathbf{n}| = 1$ was previously discussed, for example, in Refs. [13–15] with semi-classical method and Ref. [31] with a perturbative approach within WKB approximation.

B. Spin-dependent momentum distribution

We analytically compute the momentum distribution of electrons $n^{(-)}$ and positrons $n^{(+)}$ produced from the vacuum in the presence of the external field A_μ (3). To this end, we employ a perturbation theory in the Furry picture [20–25], in which the interaction with the strong field \bar{A}_μ is treated non-perturbatively and that with the weak perturbation \mathcal{A}_μ is treated perturbatively.

In the lowest order in the perturbation \mathcal{A}_μ , the (canonical) momentum distribution per spin s , $n_{\mathbf{p},s}^{(\mp)} \equiv d^3 N_s^{(\mp)}/d^3 \mathbf{p}^3$, is already given in Ref. [20].

$$\begin{aligned} n_{\pm\mathbf{p},s}^{(\mp)} &= \sum_{s'} \int d^3 \mathbf{p}' \left| \begin{array}{c} \text{Diagram 1} \\ + \\ \text{Diagram 2} \end{array} \right|^2 \\ &= \sum_{s'} \int d^3 \mathbf{p}' \left| \int d^3 \mathbf{x}_\pm \psi_{\mathbf{p},s}^{\text{out}\dagger}(x)_{\mp} \psi_{\mathbf{p}',s'}^{\text{in}}(x) \right. \\ &\quad \left. - ie \int d^4 x_\pm \bar{\psi}_{\mathbf{p},s}^{\text{out}}(x) \mathcal{A}(x)_{\mp} \psi_{\mathbf{p}',s'}^{\text{in}}(x) \right|^2, \quad (6) \end{aligned}$$

¹ One may choose $\mathcal{A}_\mu = \sin(\Omega t + \phi)/\Omega \times (0, a_1, a_2, a_3)$ in order that the electric field strength \mathcal{E} does not depend on the frequency Ω as $|\mathcal{E}| \sim |\mathbf{a}|$. For this case, the Keldysh parameter reads $\gamma_K = m\Omega/|\mathbf{a}|$. Thus, the perturbation theory in the Furry picture becomes invalid for small $\Omega \lesssim |\mathbf{a}|/m$.

where the thick line represents the electron propagator fully dressed by the strong field \bar{A}_μ as

$$\begin{aligned} \text{thick line} &= \text{thin line} + \text{thin line with } \bar{A} \text{ loop} \\ &+ \text{thin line with } \bar{A} \text{ and } \bar{A} \text{ loops} + \dots \end{aligned} \quad (7)$$

Because of the dressed propagator, the positive/negative frequency mode functions defined at the asymptotic times $|x^0| \rightarrow \infty$, $\pm\psi_{\mathbf{p},s}^{\text{as}}$ (as = in and out for $x^0 \rightarrow -\infty$ and $+\infty$, respectively), are also dressed by the strong field \bar{A}_μ . Namely, $\pm\psi_{\mathbf{p},s}^{\text{as}}$ is defined as a solution of the Dirac equation under the strong field \bar{A}_μ ,

$$0 = [i\bar{\not{D}} - e\bar{A} - m] \pm\psi_{\mathbf{p},s}^{\text{as}}, \quad (8)$$

with boundary conditions

$$\lim_{x^0 \rightarrow -\infty} \pm\psi_{\mathbf{p},s}^{\text{in}} \propto e^{i\mathbf{p}\cdot\mathbf{x}} e^{\mp i\omega_{\mathbf{p}} x^0}, \quad (9a)$$

$$\lim_{x^0 \rightarrow +\infty} \pm\psi_{\mathbf{p},s}^{\text{out}} \propto e^{i\mathbf{p}\cdot\mathbf{x}} e^{\mp i\omega_{\mathbf{p}} x^0}, \quad (9b)$$

(i.e., plane wave at the asymptotic times $x^0 \rightarrow \pm\infty$) and normalization

$$\int d^3\mathbf{x} \pm\psi_{\mathbf{p},s}^{\text{as}\dagger}(x) \pm\psi_{\mathbf{p}',s'}^{\text{as}}(x) = \delta_{ss'} \delta^3(\mathbf{p} - \mathbf{p}'), \quad (10a)$$

$$\int d^3\mathbf{x} \pm\psi_{\mathbf{p},s}^{\text{as}\dagger}(x) \mp\psi_{\mathbf{p}',s'}^{\text{as}}(x) = 0. \quad (10b)$$

We note that, in the presence of the strong field \bar{A}_μ , one has to take care of the distinction between the in- and out-state mode functions $\pm\psi_{\mathbf{p},s}^{\text{in/out}}$. This is because the non-perturbative interaction due to \bar{A}_μ mixes up the positive and negative frequency modes (i.e., particle and anti-particle modes) during the time-evolution, and thus $\pm\psi_{\mathbf{p},s}^{\text{in/out}}$ are no longer the same.

One can carry out the integrations in Eq. (6) for the present field configuration (i.e., constant electric field (4) superimposed by a monochromatic wave (5)). Note that this calculation can be done exactly without any use of approximations such as the WKB method (e.g. [21, 22, 31]). We put the detailed calculations in Appendix A. We find

$$\begin{aligned} n_{\pm\mathbf{p},s}^{(\mp)} &= \frac{V}{(2\pi)^3} \exp\left[-\pi \frac{m^2 + p_\perp^2}{e\bar{E}}\right] \\ &\times \left[1 + e \times i\pi e^{i(\phi - \frac{\Omega p_3}{eE})} \left\{ \frac{p_\perp a_\perp}{e\bar{E}} \cos(\theta_{\mathbf{p}} - \theta_{\mathbf{a}}) \text{Re} \left[e^{-i\frac{\Omega^2}{4e\bar{E}}} {}_1\tilde{F}_1 \left(1 - i\frac{m^2 + p_\perp^2}{2e\bar{E}}; 1; i\frac{\Omega^2}{2e\bar{E}} \right) \right] \right. \right. \\ &\quad + \sigma \frac{p_\perp a_\perp}{e\bar{E}} \sin(\theta_{\mathbf{p}} - \theta_{\mathbf{a}}) \text{Im} \left[e^{-i\frac{\Omega^2}{4e\bar{E}}} {}_1\tilde{F}_1 \left(1 - i\frac{m^2 + p_\perp^2}{2e\bar{E}}; 1; i\frac{\Omega^2}{2e\bar{E}} \right) \right] \\ &\quad \left. \left. - ia_3 \frac{\Omega}{e\bar{E}} \frac{m^2 + p_\perp^2}{2e\bar{E}} \text{Re} \left[e^{-i\frac{\Omega^2}{4e\bar{E}}} {}_1\tilde{F}_1 \left(1 - i\frac{m^2 + p_\perp^2}{2e\bar{E}}; 2; i\frac{\Omega^2}{2e\bar{E}} \right) \right] \right\} \right]^2 \\ &+ e^2 \times \pi^2 \frac{m^2}{e\bar{E}} \frac{a_\perp^2}{e\bar{E}} \left| \text{Im} \left[e^{-i\frac{\Omega^2}{4e\bar{E}}} {}_1\tilde{F}_1 \left(1 - i\frac{m^2 + p_\perp^2}{2e\bar{E}}; 1; i\frac{\Omega^2}{2e\bar{E}} \right) \right] \right|^2, \end{aligned} \quad (11)$$

where $\sigma \equiv +1$ (-1) for spin up $s = \uparrow$ (down $s = \downarrow$) with respect to the x^3 -axis and ${}_1\tilde{F}_1(a; b; z) \equiv {}_1F_1(a; b; z)/\Gamma(b)$ is the regularized hypergeometric function. We also introduced $p_\perp, a_\perp, \theta_{\mathbf{p}}, \theta_{\mathbf{a}}$ as

$$\begin{aligned} p_1 &= p_\perp \cos \theta_{\mathbf{p}}, \quad p_2 = p_\perp \sin \theta_{\mathbf{p}}, \\ a_1 &= a_\perp \cos \theta_{\mathbf{a}}, \quad a_2 = a_\perp \sin \theta_{\mathbf{a}}. \end{aligned} \quad (12)$$

We emphasize here that the momentum distribution (11) explicitly depends on spin s (the second term in the curly brackets). That is, the Schwinger mechanism becomes spin-dependent if one superimposes weak perturbations on top of a strong field. Notice that the Schwinger mechanism without perturbations

or the purely perturbative particle production from the monochromatic wave alone² is insensitive to spin; only when there exist both, the spin-dependent term appears. To see this explicitly, let us consider some limits of the momentum distribution (11). In the absence of the perturbation ($e \rightarrow 0$ with $e\bar{E} \neq 0$), only the first term in

² In general, the perturbative particle production can be spin-dependent for general field configurations such as a rotating field [26]. What we would like to emphasize here is that even if the perturbation alone is insensitive to spin, the mutual assistance between the strong field and the perturbation results in the spin-dependent particle production.

Eq. (6) survives and the momentum distribution (11) can be simplified as

$$n_{\pm\mathbf{p},s}^{(\mp)} \xrightarrow{e \rightarrow 0, e\bar{E} \neq 0} \frac{V}{(2\pi)^3} \exp \left[-\pi \frac{m^2 + p_{\perp}^2}{e\bar{E}} \right]. \quad (13)$$

This is nothing but the Schwinger formula for a constant electric field (1) [3], and the production is independent of spin s . On the other hand, in the absence of the strong field ($\bar{E} \rightarrow 0$), the particle production process becomes purely perturbative and the perturbation theory in the Furry picture is trivially reduced to the standard perturbation theory without strong fields [30, 32]. In this limit, only the second term in Eq. (6) survives and the momentum distribution (11) becomes

$$\begin{aligned} n_{\pm\mathbf{p},s}^{(\mp)} \xrightarrow{\bar{E} \rightarrow 0} & VT \frac{e^2}{16\pi^2} \delta(\Omega - 2\omega_{\mathbf{p}}) \\ & \times \left[\cos(\theta_{\mathbf{p}} - \theta_{\mathbf{a}}) \frac{p_{\perp} a_{\perp}}{\sqrt{m^2 + p_{\perp}^2}} \frac{p_3}{\omega_{\mathbf{p}}} \right. \\ & \quad \left. - a_3 \frac{\sqrt{m^2 + p_{\perp}^2}}{\omega_{\mathbf{p}}} \right]^2 + \frac{m^2}{m^2 + p_{\perp}^2} a_{\perp}^2 \\ & \quad + \left[\sin(\theta_{\mathbf{p}} - \theta_{\mathbf{a}}) \frac{p_{\perp} a_{\perp}}{\sqrt{m^2 + p_{\perp}^2}} \right]^2, \quad (14) \end{aligned}$$

where $\omega_{\mathbf{p}} \equiv \sqrt{m^2 + \mathbf{p}^2}$ is the on-shell energy and T is the whole time interval. Again, the production is independent of spin s . Therefore, we conclude that the spin-dependence arises because of the mutual assistance between the strong field and the weak perturbation.

The spin-dependent term is proportional to $\mathbf{e}_{x,3} \cdot (\mathbf{p} \times \mathbf{a})$, i.e., the spin-dependence appears only if the emission direction of the particle has a component perpendicular to both the strong and weak electric fields. Intuitively, this is because that a particle with transverse momentum effectively feels a magnetic field in the longitudinal direction in its rest frame if there is an electric field in the transverse direction in the observer frame.

C. Spin-imbalance

We quantify the spin-imbalance by the difference between the production number of spin up and down particles as

$$\Delta n_{\mathbf{p}}^{(\mp)} \equiv n_{\mathbf{p},\uparrow}^{(\mp)} - n_{\mathbf{p},\downarrow}^{(\mp)}. \quad (15)$$

From the momentum distribution (11), the spin-imbalance $\Delta n_{\mathbf{p}}^{(\mp)}$ can be evaluated as

$$\begin{aligned} \Delta n_{\mathbf{p}}^{(\mp)} = & \frac{V}{2\pi^2} \exp \left[-\pi \frac{m^2 + p_{\perp}^2}{e\bar{E}} \right] \frac{ea_{\perp}p_{\perp}}{e\bar{E}} \text{Im} \left[e^{-i\frac{\Omega^2}{4e\bar{E}}} {}_1\tilde{F}_1 \left(1 - i\frac{m^2 + p_{\perp}^2}{2e\bar{E}}; 1; i\frac{\Omega^2}{2e\bar{E}} \right) \right] \\ & \times \left\{ \mp \sin \left(\phi \mp \frac{\Omega p_3}{e\bar{E}} \right) \sin(\theta_{\mathbf{p}} - \theta_{\mathbf{a}}) + \frac{\pi}{2} \frac{ea_{\perp}p_{\perp}}{e\bar{E}} \text{Re} \left[e^{-i\frac{\Omega^2}{4e\bar{E}}} {}_1\tilde{F}_1 \left(1 - i\frac{m^2 + p_{\perp}^2}{2e\bar{E}}; 1; i\frac{\Omega^2}{2e\bar{E}} \right) \right] \sin(2(\theta_{\mathbf{p}} - \theta_{\mathbf{a}})) \right\}. \quad (16) \end{aligned}$$

The first term in the curly brackets appears because of the interference between the two diagrams in Eq. (6), and the second term comes solely from the second diagram.

The ϕ -dependence of the spin-imbalance $\Delta n_{\mathbf{p}}^{(\mp)}$ always appears with the factor $\mp \Omega p_3 / e\bar{E}$. Intuitively, the particle production becomes the most efficient at the instant when the longitudinal kinetic momentum $P_3 = p_3 \pm e\bar{E}x^0$ (+, - for an electron and a positron, respectively) is vanishing, at which the energy cost of the production becomes the smallest [20, 33]. Therefore, the value of the weak field at $x^0 = \mp p_3 / e\bar{E}$ becomes important, at which the phase of the weak field (5) reads $\phi \mp \Omega p_3 / e\bar{E}$.

The spin-imbalance $\Delta n_{\mathbf{p}}^{(\mp)}$ shows non-trivial dependence in Ω . For small $\Omega \lesssim \sqrt{e\bar{E}}$ and $\sqrt{m^2 + p_{\perp}^2}$, $\Delta n_{\mathbf{p}}^{(\mp)}$ is proportional to Ω^2 as

$$\Delta n_{\mathbf{p}}^{(\mp)} \xrightarrow{\Omega \rightarrow 0} \frac{V}{2\pi^2} \exp \left[-\pi \frac{m^2 + p_{\perp}^2}{e\bar{E}} \right] \frac{ea_{\perp}p_{\perp}}{e\bar{E}} \frac{\Omega^2}{4e\bar{E}} \left\{ \mp \sin \left(\phi \mp \frac{\Omega p_3}{e\bar{E}} \right) \sin(\theta_{\mathbf{p}} - \theta_{\mathbf{a}}) + \frac{\pi}{2} \frac{ea_{\perp}p_{\perp}}{e\bar{E}} \sin(2(\theta_{\mathbf{p}} - \theta_{\mathbf{a}})) \right\}. \quad (17)$$

On the other hand, for large $\Omega \gtrsim \sqrt{e\bar{E}}, \sqrt{m^2 + p_{\perp}^2}$, the magnitude of $\Delta n_{\mathbf{p}}^{(\mp)}$ becomes constant but it oscillates rapidly

in Ω as

$$\begin{aligned} \Delta n_{\mathbf{p}}^{(\mp)} \xrightarrow{\Omega \rightarrow \infty} & \frac{1}{\pi^3} \exp \left[-\pi \frac{m^2 + p_{\perp}^2}{2e\bar{E}} \right] \sqrt{1 - \exp \left[-\pi \frac{m^2 + p_{\perp}^2}{e\bar{E}} \right]} \frac{\sqrt{\pi}}{2} \sqrt{\frac{e\bar{E}}{m^2 + p_{\perp}^2} \frac{ea_{\perp}p_{\perp}}{e\bar{E}}} \sin \varphi \\ & \times \left[\mp \sin \left(\phi \mp \frac{\Omega p_3}{e\bar{E}} \right) \sin(\theta_{\mathbf{p}} - \theta_{\mathbf{a}}) \right. \\ & \left. + \exp \left[+\pi \frac{m^2 + p_{\perp}^2}{2e\bar{E}} \right] \sqrt{1 - \exp \left[-\pi \frac{m^2 + p_{\perp}^2}{e\bar{E}} \right]} \frac{\sqrt{\pi}}{2} \sqrt{\frac{e\bar{E}}{m^2 + p_{\perp}^2} \frac{ea_{\perp}p_{\perp}}{e\bar{E}}} \cos \varphi \sin(2(\theta_{\mathbf{p}} - \theta_{\mathbf{a}})) \right], \end{aligned} \quad (18)$$

where the phase factor $\varphi = \varphi(\Omega)$ determines the frequency of the oscillation as

$$\varphi \equiv \frac{\Omega^2}{4e\bar{E}} - \frac{m^2 + p_{\perp}^2}{2e\bar{E}} \ln \frac{\Omega^2}{2e\bar{E}} - i \ln \left[\frac{\Gamma \left(1 + i \frac{m^2 + p_{\perp}^2}{2e\bar{E}} \right)}{\left| \Gamma \left(1 + i \frac{m^2 + p_{\perp}^2}{2e\bar{E}} \right) \right|} \right]. \quad (19)$$

The oscillation in Ω is reminiscent of the Franz-Keldysh oscillation, which originates from oscillating distribution of electrons in the Dirac sea due to quantum reflection by the band gap [20]. Note that $\Delta n_{\mathbf{p}}^{(\mp)}$ for large Ω is no longer suppressed exponentially by $|e\bar{E}|^{-1}$ because the second term in the curly brackets in Eq. (18) is exponentially large so that it cancels with the suppression factor. This is because the perturbative effect dominates the production for large Ω .

As the two terms in Eq. (18) have distinct $\theta_{\mathbf{p}}$ -dependence, the $\theta_{\mathbf{p}}$ -dependence of the spin-imbalance $\Delta n_{\mathbf{p}}^{(\mp)}$ is determined by which term is dominant. Namely, $\Delta n_{\mathbf{p}}^{(\mp)}$ becomes proportional to $\sin(\theta_{\mathbf{p}} - \theta_{\mathbf{a}})$ ($\sin(2(\theta_{\mathbf{p}} - \theta_{\mathbf{a}}))$) if the first (second) term dominates the production: For supercritical field strength $e\bar{E} \gtrsim m^2 + p_{\perp}^2$, the dimensionless quantity $a_{\perp}p_{\perp}/\bar{E}$ (i.e., the strength of the effective magnetic field $\propto \mathbf{p} \times \mathbf{a}$ divided by the original electric field strength \bar{E}) determines the relative size between the two terms. Thus, the first and the second term becomes dominant for $a_{\perp}p_{\perp}/\bar{E} \lesssim 1$ and $a_{\perp}p_{\perp}/\bar{E} \gtrsim 1$, respectively. On the other hand, for subcritical field strength $e\bar{E} \lesssim m^2 + p_{\perp}^2$, $a_{\perp}p_{\perp}/\bar{E}$ determines the relative size only when the frequency Ω is small. When Ω becomes large, the exponential factor becomes important. Thus, the second term dominates the spin-imbalance provided that $a_{\perp}p_{\perp}/\bar{E}$ is not exponentially small. Note that the first term vanishes if one

integrates $\Delta n_{\mathbf{p}}^{(\mp)}$ over the longitudinal momentum p_3 as

$$\begin{aligned} & \int dp_3 \Delta n_{\mathbf{p}}^{(\mp)} \\ & = \frac{VT}{4\pi} e\bar{E} \exp \left[-\pi \frac{m^2 + p_{\perp}^2}{e\bar{E}} \right] \left| \frac{a_{\perp}p_{\perp}}{\bar{E}} \right|^2 \\ & \quad \times \text{Im} \left[e^{-i \frac{\Omega^2}{4e\bar{E}}} {}_1\tilde{F}_1 \left(1 - i \frac{m^2 + p_{\perp}^2}{2e\bar{E}}; 1; i \frac{\Omega^2}{2e\bar{E}} \right) \right] \\ & \quad \times \text{Re} \left[e^{-i \frac{\Omega^2}{4e\bar{E}}} {}_1\tilde{F}_1 \left(1 - i \frac{m^2 + p_{\perp}^2}{2e\bar{E}}; 1; i \frac{\Omega^2}{2e\bar{E}} \right) \right] \\ & \quad \times \sin(2(\theta_{\mathbf{p}} - \theta_{\mathbf{a}})), \end{aligned} \quad (20)$$

where we used $\int dp_3 = e\bar{E}T$ [33]. Thus, the $\theta_{\mathbf{p}}$ -dependence of the spin-imbalance in the transverse distribution $\int dp_3 (n_{\mathbf{p},\uparrow}^{(\mp)} - n_{\mathbf{p},\downarrow}^{(\mp)})$ is independent of the parameters and is always proportional to $\sin(2(\theta_{\mathbf{p}} - \theta_{\mathbf{a}}))$.

It is evident from Eq. (16) that the spin-imbalance vanishes after $\theta_{\mathbf{p}}$ -integration. That is, the total number of spin up and down particles is the same as

$$\int d\theta_{\mathbf{p}} \Delta n_{\mathbf{p}}^{(\mp)} = 0. \quad (21)$$

This is a natural result since the vacuum is unpolarized.

III. NUMERICAL EVALUATION OF THE SPIN-IMBALANCE

In this section, we numerically study the spin-dependent Schwinger mechanism by directly solving the Dirac equation on a computer without any approximations: In Sec. III A, we first explain how to compute the spin-imbalance from a solution of the Dirac equation by using the Bogoliubov transformation technique. In Sec. III B, we present our numerical results, and discuss the spin-imbalance quantitatively. We also show that the

numerical results are in an excellent agreement with the analytical formula derived in Sec. II.

A. Formalism: the Bogoliubov transformation

We explain how to compute the spin-imbalance $\Delta n_{\mathbf{p},s}^{(\mp)}$ on a computer without relying on any approximations. Our formulation is based on the Bogoliubov transformation technique [34] including spin-dependence [35, 36].

We first introduce a gauge field configuration defined

by

$$\check{A}_\mu(x^0) \equiv \begin{cases} A_\mu(-\tau) & (x^0 < -\tau) \\ A_\mu(x^0) & (-\tau < x^0 < +\tau) \\ A_\mu(+\tau) & (+\tau < x^0) \end{cases}, \quad (22)$$

where $\tau > 0$ and A_μ is the original gauge field configuration (3)³. Notice that

$$\check{A}_\mu \xrightarrow{\tau \rightarrow \infty} A_\mu, \quad (23)$$

so that the production number by the original field A_μ can be obtained from that by \check{A}_μ with sufficiently long τ .

As \check{A}_μ becomes a pure gauge (i.e., non-interacting with $\hat{\psi}$) at $x^0 < -\tau$ and $x^0 > \tau$, one can safely expand the field operator $\hat{\psi}$ by a plane wave and canonically quantize $\hat{\psi}$ to define creation/annihilation operators at $x^0 < -\tau$ and $x^0 > \tau$ as⁴

$$\hat{\psi}(x) = \begin{cases} \sum_s \int d^3\mathbf{p} \left[u_{\mathbf{P}(-\tau),s} e^{-i\omega_{\mathbf{P}(-\tau)}x^0} \hat{a}_{\mathbf{p},s}^{(-\tau)} + v_{\mathbf{P}(-\tau),s} e^{+i\omega_{\mathbf{P}(-\tau)}x^0} \hat{b}_{-\mathbf{p},s}^{(-\tau)\dagger} \right] \frac{e^{i\mathbf{p}\cdot\mathbf{x}}}{(2\pi)^{3/2}} & \text{for } x^0 < -\tau \\ \sum_s \int d^3\mathbf{p} \left[u_{\mathbf{P}(+\tau),s} e^{-i\omega_{\mathbf{P}(+\tau)}x^0} \hat{a}_{\mathbf{p},s}^{(+\tau)} + v_{\mathbf{P}(+\tau),s} e^{+i\omega_{\mathbf{P}(+\tau)}x^0} \hat{b}_{-\mathbf{p},s}^{(+\tau)\dagger} \right] \frac{e^{i\mathbf{p}\cdot\mathbf{x}}}{(2\pi)^{3/2}} & \text{for } x^0 > +\tau \end{cases}, \quad (24)$$

where, as before, \mathbf{p} is (canonical) momentum, $s = \uparrow, \downarrow$ is spin, and $\omega_{\mathbf{p}} = \sqrt{m^2 + \mathbf{p}^2}$ is the on-shell energy. We also introduced $\check{\mathbf{A}} \equiv (\check{A}^1, \check{A}^2, \check{A}^3)$, $\check{\mathbf{P}} \equiv \mathbf{p} - e\check{\mathbf{A}}$, and $u_{\mathbf{p},s}, v_{\mathbf{p},s}$ represent the Dirac spinors such that

$$0 = [\gamma^0 \omega_{\mathbf{p}} - \boldsymbol{\gamma} \cdot \mathbf{p} - m] u_{\mathbf{p},s}, \quad (25a)$$

$$0 = [\gamma^0 \omega_{\mathbf{p}} + \boldsymbol{\gamma} \cdot \mathbf{p} + m] v_{\mathbf{p},s} \quad (25b)$$

with $\boldsymbol{\gamma} \equiv (\gamma^1, \gamma^2, \gamma^3)$ and normalization

$$u_{\mathbf{p},s}^\dagger u_{\mathbf{p},s'} = v_{\mathbf{p},s}^\dagger v_{\mathbf{p},s'} = \delta_{ss'}, \quad u_{\mathbf{p},s}^\dagger v_{\mathbf{p},s'} = 0. \quad (26)$$

The creation/annihilation operators satisfy the following

anti-commutation relations

$$\{a_{\mathbf{p},s}^{(\pm\tau)\dagger}, a_{\mathbf{p}',s'}^{(\pm\tau)}\} = \{b_{\mathbf{p},s}^{(\pm\tau)\dagger}, b_{\mathbf{p}',s'}^{(\pm\tau)}\} = \delta_{ss'} \delta^3(\mathbf{p} - \mathbf{p}'), \quad (27a)$$

$$(\text{others}) = 0. \quad (27b)$$

An important point here is that the creation/annihilation operators at $x^0 = +\tau$ and those at $x^0 = -\tau$ are inequivalent because of the interaction with the electromagnetic field \check{A}_μ during the time-evolution $-\tau < x^0 < \tau$. The inequivalence can be expressed in terms of a Bogoliubov transformation. To see this, we first expand the field operator $\hat{\psi}$ in terms of the creation/annihilation operators at $x^0 < -\tau$ as

$$\hat{\psi}(x) = \sum_s \int d^3\mathbf{p} \left[U_{\mathbf{p},s}(x^0) \hat{a}_{\mathbf{p},s}^{(-\tau)} + V_{\mathbf{p},s}(x^0) \hat{b}_{-\mathbf{p},s}^{(-\tau)} \right] \frac{e^{i\mathbf{p}\cdot\mathbf{x}}}{(2\pi)^{3/2}}. \quad (28)$$

The time-evolution of the mode functions U, V is determined by the Dirac equation

$$0 = \left[i\gamma^0 \partial_{x^0} - \boldsymbol{\gamma} \cdot (\mathbf{p} - e\check{\mathbf{A}}) - m \right] \begin{pmatrix} U_{\mathbf{p},s} \\ V_{\mathbf{p},s} \end{pmatrix}. \quad (29)$$

The initial condition for the mode functions U, V is fixed by the first line of Eq. (24) as

$$U_{\mathbf{p},s}(-\tau) = u_{\mathbf{P}(-\tau),s} e^{-i\omega_{\mathbf{P}(-\tau)}x^0}, \quad (30a)$$

$$V_{\mathbf{p},s}(-\tau) = v_{\mathbf{P}(-\tau),s} e^{+i\omega_{\mathbf{P}(-\tau)}x^0}. \quad (30b)$$

³ In general, one may define \check{A}_μ as $\check{A}_\mu(x^0) \equiv A_\mu(x^0)f(x^0)$ with f being a support that has a smooth behavior at the boundary $|x^0| = \tau$. In this paper, we consider the simplest support $f = 0$ for $|x^0| > \tau$ and 1 for $|x^0| < \tau$. This is because the boundary effects in the production number can be neglected in the limit of $\tau \rightarrow \infty$, and the final formulas (37a) and (37b) are insensitive to the choice of f .

⁴ Only when the gauge field becomes a pure gauge, one can define creation/annihilation operators in a well-defined manner. In other words, one cannot uniquely define creation/annihilation operators in the presence of non-vanishing electromagnetic field because the interaction between $\hat{\psi}$ and the field mixes up particle and anti-particle modes. For such a case, one has to make an additional assumption (e.g. adiabatic particle picture [37]) to define the operators.

Note that because of this initial condition, the mode functions U, V satisfy the same normalization condition for u, v as

$$U_{\mathbf{p},s}^\dagger U_{\mathbf{p},s'} = V_{\mathbf{p},s}^\dagger V_{\mathbf{p},s'} = \delta_{ss'}, \quad U_{\mathbf{p},s}^\dagger V_{\mathbf{p},s'} = 0. \quad (31)$$

Now, we are ready to express $\hat{a}_{\mathbf{p},s}^{(+\tau)}, \hat{b}_{-\mathbf{p},s}^{(+\tau)\dagger}$ in terms of a Bogoliubov transformation of $\hat{a}_{\mathbf{p},s}^{(-\tau)}, \hat{b}_{-\mathbf{p},s}^{(-\tau)\dagger}$. By noting the second line of Eq. (24), we find

$$\begin{aligned} \begin{pmatrix} \hat{a}_{\mathbf{p},s}^{(+\tau)} \\ \hat{b}_{-\mathbf{p},s}^{(+\tau)\dagger} \end{pmatrix} &= \int d^3 \mathbf{x} \frac{e^{-i\mathbf{p}\cdot\mathbf{x}}}{(2\pi)^{3/2}} \begin{pmatrix} u_{\mathbf{P}(+\tau),s}^\dagger e^{+i\omega_{\mathbf{P}(+\tau)}\tau} \\ v_{\mathbf{P}(+\tau),s}^\dagger e^{-i\omega_{\mathbf{P}(+\tau)}\tau} \end{pmatrix} \hat{\psi}(+\tau) \\ &= \sum_{s'} \begin{pmatrix} u_{\mathbf{P}(+\tau),s}^\dagger U_{\mathbf{p},s'}(\tau) e^{+i\omega_{\mathbf{P}(+\tau)}\tau} & u_{\mathbf{P}(+\tau),s}^\dagger V_{\mathbf{p},s'}(\tau) e^{+i\omega_{\mathbf{P}(+\tau)}\tau} \\ v_{\mathbf{P}(+\tau),s}^\dagger U_{\mathbf{p},s'}(\tau) e^{-i\omega_{\mathbf{P}(+\tau)}\tau} & v_{\mathbf{P}(+\tau),s}^\dagger V_{\mathbf{p},s'}(\tau) e^{-i\omega_{\mathbf{P}(+\tau)}\tau} \end{pmatrix} \begin{pmatrix} \hat{a}_{\mathbf{p},s'}^{(-\tau)} \\ \hat{b}_{-\mathbf{p},s'}^{(-\tau)\dagger} \end{pmatrix}. \end{aligned} \quad (32)$$

Notice that the matrix elements is not diagonal in the spin space $\not\propto \delta_{ss'}$ if the external field \hat{A} affects the spin state during the time-evolution.

Now, we can evaluate the spin-dependent production number of electrons and positrons $n^{(\mp)}$ produced from the vacuum under the external field A_μ based on Eq. (32). To this end, we first define a vacuum state at $x^0 < -\tau$ as

$$0 = \begin{pmatrix} \hat{a}_{\mathbf{p},s}^{(-\tau)} \\ \hat{b}_{-\mathbf{p},s}^{(-\tau)\dagger} \end{pmatrix} |\text{vac}; -\tau\rangle \text{ for any } \mathbf{p}, s. \quad (33)$$

Then, one can directly evaluate the vacuum expectation value of the number operator at $x^0 > \tau$ (i.e, the production number under \hat{A}_μ) as

$$\begin{aligned} \check{n}_{\mathbf{p},s}^{(-)} &\equiv \frac{\langle \text{vac}; -\tau | \hat{a}_{\mathbf{p},s}^{(+\tau)\dagger} \hat{a}_{\mathbf{p},s}^{(+\tau)} | \text{vac}; -\tau \rangle}{\langle \text{vac}; -\tau | \text{vac}; -\tau \rangle} \\ &= \frac{V}{(2\pi)^3} \sum_{s'} \left| u_{\mathbf{p}-e\hat{A}(\tau),s}^\dagger V_{\mathbf{p},s'}(\tau) \right|^2, \end{aligned} \quad (34)$$

$$\begin{aligned} \check{n}_{\mathbf{p},s}^{(+)} &\equiv \frac{\langle \text{vac}; -\tau | \hat{b}_{\mathbf{p},s}^{(+\tau)\dagger} \hat{b}_{\mathbf{p},s}^{(+\tau)} | \text{vac}; -\tau \rangle}{\langle \text{vac}; -\tau | \text{vac}; -\tau \rangle} \\ &= \frac{V}{(2\pi)^3} \sum_{s'} \left| v_{-\mathbf{p}-e\hat{A}(\tau),s}^\dagger U_{-\mathbf{p},s'}(\tau) \right|^2, \end{aligned} \quad (35)$$

where the use is made of $\delta^3(\mathbf{p} = \mathbf{0}) = V/(2\pi)^3$. Therefore, as noted at Eq. (23), the production number $n^{(\mp)}$ by A_μ can be obtained by taking $\tau \rightarrow \infty$ limit of $\check{n}^{(\mp)}$ as

$$n_{\mathbf{p},s}^{(\mp)} = \lim_{\tau \rightarrow \infty} \check{n}_{\mathbf{p},s}^{(\mp)}. \quad (36)$$

From Eq. (36), we arrive at a formula for the spin-

imbalance $\Delta n_{\mathbf{p}}^{(\mp)}$ as

$$\Delta n_{\mathbf{p}}^{(-)} = \lim_{\tau \rightarrow \infty} \sum_s \left[\left| u_{\mathbf{p}-e\mathbf{A}(\tau),\uparrow}^\dagger V_{\mathbf{p},s}(\tau) \right|^2 - \left| u_{\mathbf{p}-e\mathbf{A}(\tau),\downarrow}^\dagger V_{\mathbf{p},s}(\tau) \right|^2 \right], \quad (37a)$$

$$\Delta n_{\mathbf{p}}^{(+)} = \lim_{\tau \rightarrow \infty} \sum_s \left[\left| v_{-\mathbf{p}-e\mathbf{A}(\tau),\uparrow}^\dagger U_{-\mathbf{p},s}(\tau) \right|^2 - \left| v_{-\mathbf{p}-e\mathbf{A}(\tau),\downarrow}^\dagger U_{-\mathbf{p},s}(\tau) \right|^2 \right], \quad (37b)$$

Notice that the formula is exact since we used no approximations in its derivation, and can be evaluated on a computer just by solving the Dirac equation (29).

B. Numerical results

We present some numerical results based on the formalism explained in Sec. III B, and discuss the spin-dependent Schwinger mechanism quantitatively. We also show that the analytical formula (16) reproduces the numerical results very well.

Note that we present the results for electrons only. With explicit numerical calculation, we find that positron's distribution can be obtained from electron's one just by flipping the sign of the momentum \mathbf{p} . This is consistent with the analytical formula (16), and with physical intuition that electrons and positrons are created as a pair, whose total momentum is zero.

1. Ω -dependence

Figure 1 shows the spin-imbalance $\Delta n_{\mathbf{p}}^{(-)}$ as a function of the azimuthal angle $\theta_{\mathbf{p}}$ and the frequency Ω . In addition, its comparison with the analytical formula (16) is displayed in Fig. 2, which clearly shows that Eq. (16) is in an excellent agreement with the numerical results. Here,

we considered the following parameter set as a demonstration: $e\bar{E}/m^2 = 0.5$, $a_{\perp}/m = 0.01$, $a_3/m = 0$, $p_{\perp}/m = 1$, $p_3/m = 0$, $\phi = 1$. Also, we took $m\tau = 100$. We carefully checked that this τ is sufficiently large and the results are insensitive to its values. The numerical accuracy of the results is carefully checked by the normalization condition of U, V (31). Note that we checked that the results are insensitive to the magnitude of the longitudinal perturbation a_3 as expected from the analytical formula (16). We also checked that results with non-zero p_3 is reproduced very well by shifting the phase ϕ as $\phi \rightarrow \phi - \Omega p_3/e\bar{E}$ as Eq. (16) suggests.

The figures show that the spin-imbalance is an oscillating function of $\theta_{\mathbf{p}}$ and Ω , but its oscillating behavior becomes quite different depending on the size of the frequency Ω :

For small frequency $\Omega \lesssim \sqrt{m^2 + p_{\perp}^2}, \sqrt{e\bar{E}}$, the spin-imbalance is just a monotonic function of Ω as $|\Delta n_{\mathbf{p}}^{(-)}| \propto \Omega^2$. This is because the production numbers, $n_{\mathbf{p},\uparrow}^{(-)}$ and $n_{\mathbf{p},\downarrow}^{(-)}$, are enhanced by the dynamically assisted Schwinger mechanism, so that their absolute difference $|\Delta n_{\mathbf{p}}^{(-)}|$ also increases. The azimuthal angle distribution is determined by the strength of the effective magnetic field $ea_{\perp}p_{\perp}/e\bar{E}$ (see Eq. (17)). For the present parameter choice, $ea_{\perp}p_{\perp}/e\bar{E} = 0.02 \ll 1$, so that $\Delta n_{\mathbf{p}}^{(-)} \propto \sin(\theta_{\mathbf{p}} - \theta_{\mathbf{a}})$. One can change the $\theta_{\mathbf{p}}$ -dependence by, for example, increasing $p_{\perp}/\sqrt{e\bar{E}}$. For this case, $\Delta n_{\mathbf{p}}^{(-)} \propto \sin(2(\theta_{\mathbf{p}} - \theta_{\mathbf{a}}))$ holds, but the spin-imbalance is suppressed strongly by the exponential factor $\sim \exp[-\pi(m^2 + p_{\perp}^2)/e\bar{E}]$.

For large frequency $\Omega \gtrsim \sqrt{m^2 + p_{\perp}^2}, \sqrt{e\bar{E}}$, the spin-imbalance oscillates in Ω . The oscillation becomes stronger with increasing Ω , which is a reminiscent of the Franz-Keldysh oscillation [20]. The frequency of the oscillation is reproduced very well by the phase factor $\varphi \propto \Omega^2 + \mathcal{O}(\Omega^0)$ (see Eq. (19)). Notice that the $\theta_{\mathbf{p}}$ -dependence is changed from $\Delta n_{\mathbf{p}}^{(-)} \propto \sin(\theta_{\mathbf{p}} - \theta_{\mathbf{a}})$ to $\Delta n_{\mathbf{p}}^{(-)} \propto \sin(2(\theta_{\mathbf{p}} - \theta_{\mathbf{a}}))$. This occurs for subcritical field strength $e\bar{E} \lesssim m^2 + p_{\perp}^2$ because the interference term (i.e., the first term) in Eq. (18) becomes exponentially suppressed compared to the perturbative term (i.e., the second term). For supercritical field strength $e\bar{E} \gtrsim m^2 + p_{\perp}^2$, the spin-imbalance shows up the same $\theta_{\mathbf{p}}$ -dependence as the low-frequency case $\Delta n_{\mathbf{p}}^{(-)} \propto \sin(\theta_{\mathbf{p}} - \theta_{\mathbf{a}})$ because the interference term is free from the exponential suppression and the same dimensionless quantity $ea_{\perp}p_{\perp}/e\bar{E}$ determines the angular dependence.

2. p_{\perp} -dependence

Figures 3 and 4 show the spin-imbalance $\Delta n_{\mathbf{p}}^{(-)}$ as a function of the azimuthal angle $\theta_{\mathbf{p}}$ and the transverse momentum p_{\perp} , and its comparison with the analytical formula (16), respectively. The parameters are the same

as Figs. 1 and 2.

For small $\Omega \lesssim \sqrt{e\bar{E}}, \sqrt{m^2 + p_{\perp}^2}$, the spin-imbalance is suppressed exponentially as $\Delta n_{\mathbf{p}}^{(-)} \propto \exp[-\pi(m^2 + p_{\perp}^2)/e\bar{E}]$ (see Eq. (17)). Therefore, the spin-imbalance can be manifest only for small values of $p_{\perp} \lesssim \sqrt{e\bar{E}}$. The $\theta_{\mathbf{p}}$ -dependence is determined by the strength of the effective magnetic field $ea_{\perp}p_{\perp}/e\bar{E}$ (see Eq. (17)). Thus, $\theta_{\mathbf{p}}$ -dependence of the spin-imbalance changes by increasing p_{\perp} from $\Delta n_{\mathbf{p}}^{(-)} \propto \sin(\theta_{\mathbf{p}} - \theta_{\mathbf{a}})$ to $\propto \sin(2(\theta_{\mathbf{p}} - \theta_{\mathbf{a}}))$, but the latter is not manifest in Fig. 3 because of the exponential suppression.

For large $\Omega \gtrsim \sqrt{e\bar{E}}, \sqrt{m^2 + p_{\perp}^2}$, the spin-imbalance is not suppressed exponentially until $p_{\perp} \lesssim \Omega, \sqrt{e\bar{E}}$ and shows up an oscillating behavior at large p_{\perp} . The spin-imbalance is free from the exponential suppression because the perturbative term (i.e., the second term) in Eq. (18) dominates the production. The dominance of the perturbative term implies that the $\theta_{\mathbf{p}}$ -dependence is always $\Delta n_{\mathbf{p}}^{(-)} \propto \sin(2(\theta_{\mathbf{p}} - \theta_{\mathbf{a}}))$ at large p_{\perp} . The frequency of the oscillation is, roughly, independent of p_{\perp} because the phase factor φ is dominated by Ω^2 (see Eq. (19)). This is intuitively because the direction of the effective magnetic field is independent of values of p_{\perp} .

IV. SUMMARY AND DISCUSSION

We discussed electron and positron pair production from the vacuum (the Schwinger mechanism) in the presence of a strong slow electric field superimposed by a weak monochromatic electric wave as a perturbation. We argued, both analytically and numerically, that the Schwinger mechanism becomes spin-dependent if the perturbation is transverse with respect to the strong electric field. In Sec. II, we derived an analytical formula for the spin-imbalance based on a perturbation theory in the Furry picture. In Sec. III, we solved the Dirac equation numerically to evaluate the spin-imbalance exactly. We found an excellent agreement between the numerical results and the analytical formula, and showed that the spin-imbalance (i) is strongly suppressed by an exponential of the critical field strength if the frequency of the perturbation is small, while it is suppressed only weakly by powers of the critical field strength if the frequency is large enough; and (ii) exhibits non-trivial oscillating behaviors in terms of the frequency, the azimuthal angle, and the transverse momentum of produced particles.

Let us briefly discuss the implications of our results to laser experiments. Within the current laser technologies, it is difficult to create not only a very strong electric field but also a very high frequency field exceeding the electron mass scale [38]. Thus, Eq. (17) is appropriate for the current lasers, and the spin-imbalance would be suppressed exponentially by the critical field strength. It, unfortunately, implies that it is still difficult within the current laser technologies to observe the spin-imbalance. However, it is possible to optimize the field configuration so

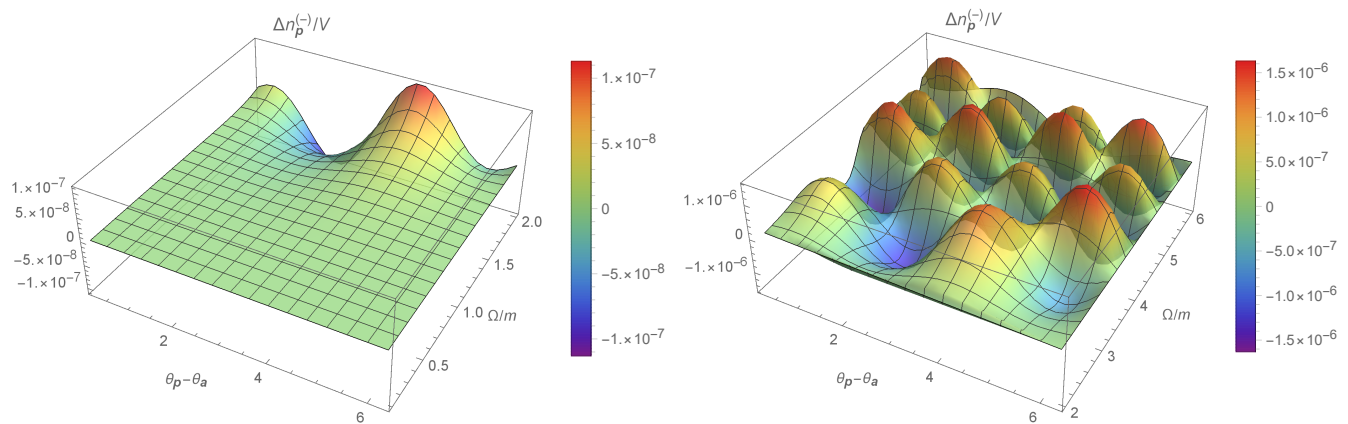


FIG. 1. (color online) The spin-imbalance $\Delta n_{\mathbf{p}}^{(-)}$ as a function of $\theta_{\mathbf{p}}$ and Ω/m . The left (right) panel shows small (large) frequency region $\Omega/m \in [0, 2]$ ($[2, 6]$). The parameters are fixed as $e\bar{E}/m^2 = 0.5$, $a_{\perp}/m = 0.01$, $a_3/m = 0$, $p_{\perp}/m = 1$, $p_3/m = 0$, $\phi = 1$, and $m\tau = 100$.

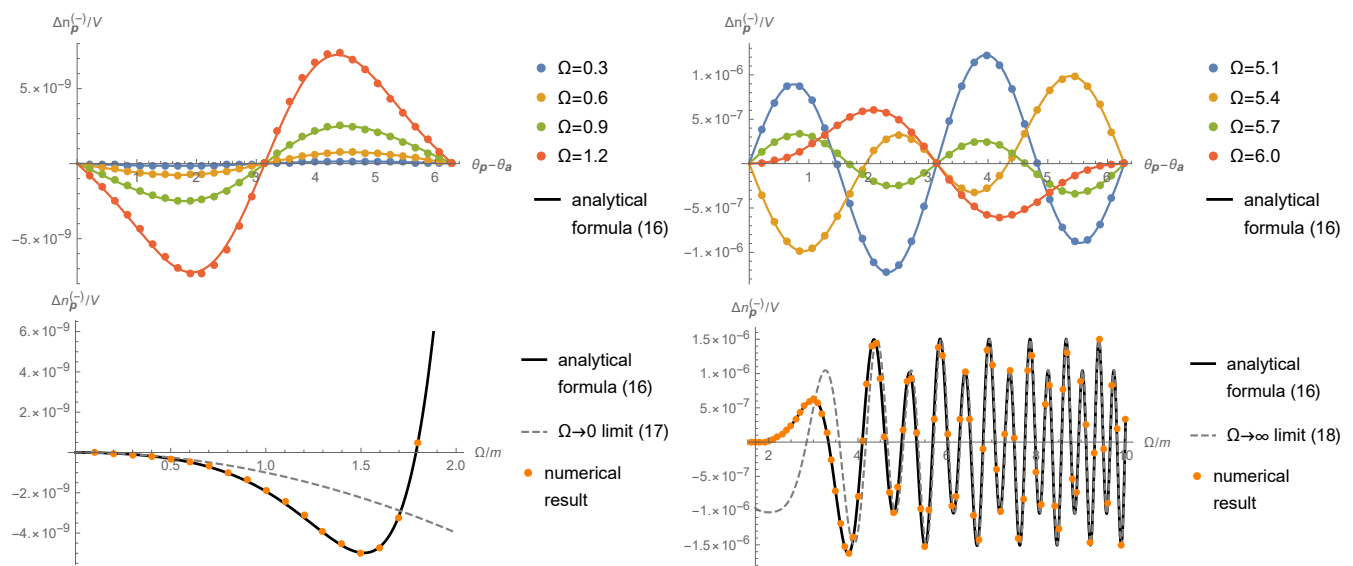


FIG. 2. (color online) Comparisons between the numerical results and the analytical formula (16). The parameters are the same as Fig. 1. [Top] $\theta_{\mathbf{p}} - \theta_{\mathbf{a}}$ -dependence for various values of $\Omega/m = 0.3, 0.6, 0.9, 1.2$ (left) and $5.1, 5.4, 5.7, 6.0$ (right). [Bottom] Ω/m -dependence for a fixed $\theta_{\mathbf{p}} - \theta_{\mathbf{a}} = \pi/4$. The left (right) panel shows small (large) frequency region $\Omega/m \in [0, 2]$ ($[2, 10]$).

as to maximize the production number [39–41]. In fact, our spin-dependent Schwinger mechanism is not limited to the monochromatic perturbation, but occurs as long as the perturbation has transverse electric field, which is not a strong constraint for the optimization procedure. It is, therefore, important and interesting for the current laser experiments to explore the optimization problem of the spin-imbalance. On the other hand, if a high frequency laser is realized in the future, the spin-imbalance is suppressed only weakly by powers of the critical field strength (see Eq. (18)), so that it should be testable in experiments. In particular, the non-trivial oscillating patterns in terms of the frequency of the perturbation, and the azimuthal angle and the transverse momentum of produced particles should serve as a fingerprint of our

spin-dependent Schwinger mechanism.

Finally, we note that laser experiments are not the only place for strong fields to appear. Strong fields naturally appear in many physical systems under extreme conditions (e.g. neutron stars, heavy-ion collisions, early Universe). For example, just after a collision of heavy ions at RHIC and LHC, there appears very strong (chromo-)electromagnetic field (sometimes called “glasma”), which is as strong as $\mathcal{O}(1 \text{ GeV})$ [42–46]. On top of the glasma, there also exist energetic jets, whose momentum scale is $\mathcal{O}(1 \sim 100 \text{ GeV})$, coming from initial hard collisions. It is widely recognized that the Schwinger mechanism due to the glasma plays an essential role in the formation of quark-gluon plasma in heavy-ion collisions [34, 36, 42, 43, 47–49], but interaction effects due to

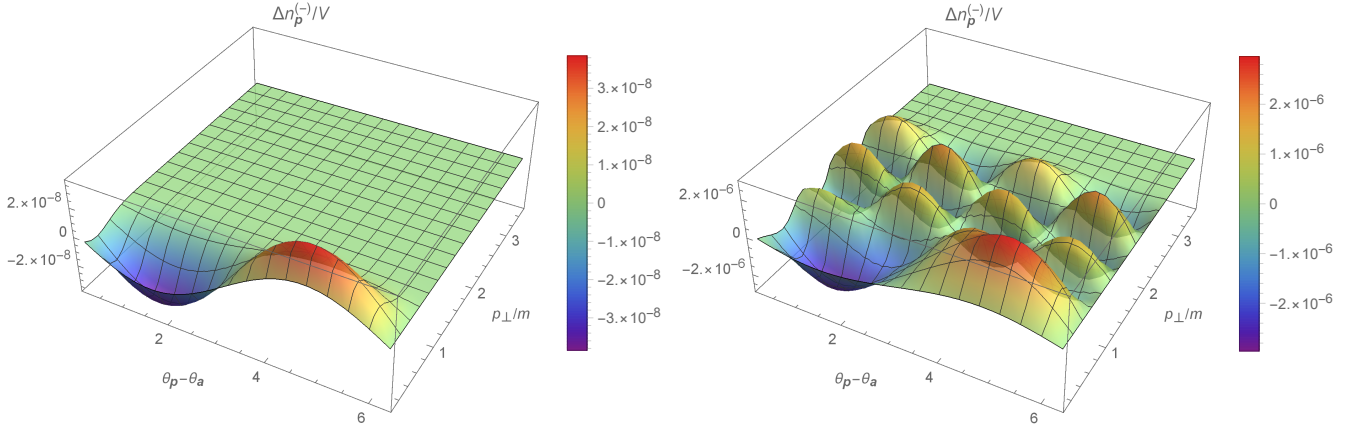


FIG. 3. (color online) The spin-imbalance $\Delta n_{\mathbf{p}}^{(-)}$ as a function of $\theta_{\mathbf{p}}$ and p_{\perp}/m for small (large) frequency $\Omega/m = 0.5$ (5.0) are displayed in the left (right) panel. The other parameters are the same as Fig. 1.

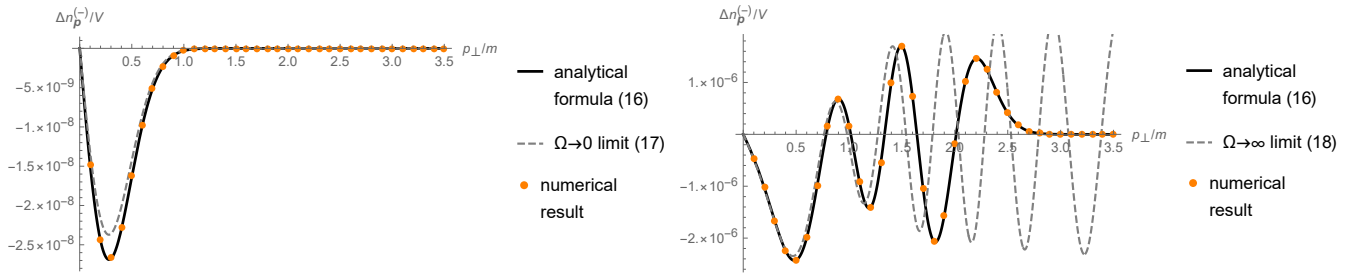


FIG. 4. (color online) Comparisons between the numerical results and the analytical formula (16) for p_{\perp} -dependence of the spin-imbalance $\Delta n_{\mathbf{p}}^{(-)}$ for $\Omega/m = 0.5$ (left) and 5.0 (right) at $\theta_{\mathbf{p}} - \theta_{\mathbf{a}} = \pi/4$. The other parameters are the same as Fig. 1.

the presence of jets have not been understood well. Our results suggest that the interaction effects leave significant impacts on the Schwinger mechanism, and may induce longitudinal spin polarization of quarks. This might contribute to the longitudinal spin-polarization observed in heavy-ion collision experiments [51, 52]. Another example is the asymmetric heavy-ion collisions, e.g., Cu + Au collisions, in which strong electric field can be generated with strength much larger than the critical field strength [53, 54]. This strong electric field points from the Au nucleus to Cu nucleus and thus if it is perturbed by charged jets it will emit electron and positron pairs with spin-imbalance in the out-of-plane direction, which may be detected by measuring the spin polarization (along the impact-parameter direction) of electron and positron moving in the direction perpendicular to the reaction plane. We will examine these possibilities in future.

ACKNOWLEDGEMENTS

H. T. would like to thank Koichi Hattori, Mamoru Matsuo, and RIKEN iTHEMS STAMP working group for useful discussions. H. T. is supported by National Natural Science Foundation in

China (NSFC) under Grants No. 11847206. X.-G. H is supported by NSFC under Grants No. 11535012 and No. 11675041.

Appendix A: Evaluation of Eq. (6)

In order to evaluate the integrals in Eq. (6), we first note that the analytical expression for the mode function $\pm\psi_{\mathbf{p},s}^{\text{as}}$ for the constant electric field configuration (4) is given by [33, 34]

$$+\psi_{\mathbf{p},s}^{\text{as}}(x) = \left[A_{\mathbf{p}}^{\text{as}}(x^0) + B_{\mathbf{p}}^{\text{as}}(x^0) \gamma^0 \frac{m + \boldsymbol{\gamma}_{\perp} \cdot \mathbf{p}_{\perp}}{\sqrt{m^2 + \mathbf{p}_{\perp}^2}} \right] \Gamma_s \frac{e^{i\mathbf{p} \cdot \mathbf{x}}}{(2\pi)^{3/2}}, \quad (\text{A1a})$$

$$-\psi_{\mathbf{p},s}^{\text{as}}(x) = \left[B_{\mathbf{p}}^{\text{as}*}(x^0) - A_{\mathbf{p}}^{\text{as}*}(x^0) \gamma^0 \frac{m + \boldsymbol{\gamma}_{\perp} \cdot \mathbf{p}_{\perp}}{\sqrt{m^2 + \mathbf{p}_{\perp}^2}} \right] \Gamma_s \frac{e^{i\mathbf{p} \cdot \mathbf{x}}}{(2\pi)^{3/2}}, \quad (\text{A1b})$$

where $\boldsymbol{\gamma}_{\perp} = (\gamma^1, \gamma^2)$, $\mathbf{p}_{\perp} = (p_1, p_2)$ is transverse momentum with respect to the direction of the electric field, and

the scalar functions $A_{\mathbf{p}}^{\text{as}}, B_{\mathbf{p}}^{\text{as}}$ are

$$\begin{cases} A_{\mathbf{p}}^{\text{in}} = e^{-\frac{i\pi}{8}} e^{-\frac{\pi\alpha_{\mathbf{p}}}{4}} \sqrt{a_{\mathbf{p}}} D_{ia_{\mathbf{p}}-1} \left(-e^{-\frac{i\pi}{4}} \xi_{\mathbf{p}}(x^0) \right) \\ B_{\mathbf{p}}^{\text{in}} = e^{+\frac{i\pi}{8}} e^{-\frac{\pi\alpha_{\mathbf{p}}}{4}} D_{ia_{\mathbf{p}}} \left(-e^{-\frac{i\pi}{4}} \xi_{\mathbf{p}}(x^0) \right) \end{cases}, \quad (\text{A2a})$$

$$\begin{cases} A_{\mathbf{p}}^{\text{out}} = e^{-\frac{i\pi}{8}} e^{-\frac{\pi\alpha_{\mathbf{p}}}{4}} D_{-ia_{\mathbf{p}}} \left(e^{\frac{i\pi}{4}} \xi_{\mathbf{p}}(x^0) \right) \\ B_{\mathbf{p}}^{\text{out}} = e^{+\frac{i\pi}{8}} e^{-\frac{\pi\alpha_{\mathbf{p}}}{4}} \sqrt{a_{\mathbf{p}}} D_{-ia_{\mathbf{p}}-1} \left(e^{\frac{i\pi}{4}} \xi_{\mathbf{p}}(x^0) \right) \end{cases}, \quad (\text{A2b})$$

with $D_{\nu}(z)$ being the parabolic cylinder function and

$$a_{\mathbf{p}} \equiv \frac{m^2 + \mathbf{p}_{\perp}^2}{2e\bar{E}}, \quad \xi_{\mathbf{p}} \equiv \sqrt{\frac{2}{e\bar{E}}} (e\bar{E}x^0 + p_3). \quad (\text{A3})$$

Γ_s are two eigenvectors of $\gamma^0\gamma^3$ with eigenvalue $+1$, and $s = \uparrow, \downarrow$ specifies spin direction with respect to the x^3 -axis. In the Dirac representation, Γ_s can be expressed as

$$\Gamma_{\uparrow} = \frac{1}{\sqrt{2}} \begin{pmatrix} 1 \\ 0 \\ 1 \\ 0 \end{pmatrix}, \quad \Gamma_{\downarrow} = \frac{1}{\sqrt{2}} \begin{pmatrix} 0 \\ 1 \\ 0 \\ -1 \end{pmatrix}. \quad (\text{A4})$$

By plugging Eqs. (A1a) and (A1b) into Eq. (6), one obtains

$$\begin{aligned} n_{\pm\mathbf{p},s}^{(\mp)} = \frac{V}{(2\pi)^3} & \left[\left| e^{-\pi a_{\mathbf{p}}} - ie \int_{-\infty}^{+\infty} \frac{dk}{2\pi} \left\{ \frac{p_1 \tilde{\mathcal{A}}_1 + p_2 \tilde{\mathcal{A}}_2}{\sqrt{m^2 + \mathbf{p}_{\perp}^2}} \times \int_{-\infty}^{+\infty} dx^0 e^{+ikx^0} [-A_{\mathbf{p}}^{\text{out}*} A_{\mathbf{p}}^{\text{in}*} + B_{\mathbf{p}}^{\text{out}*} B_{\mathbf{p}}^{\text{in}*}] \right. \right. \\ & + i\sigma \frac{-p_2 \tilde{\mathcal{A}}_1 + p_1 \tilde{\mathcal{A}}_2}{\sqrt{m^2 + \mathbf{p}_{\perp}^2}} \times \int_{-\infty}^{+\infty} dx^0 e^{+ikx^0} [A_{\mathbf{p}}^{\text{out}*} A_{\mathbf{p}}^{\text{in}*} + B_{\mathbf{p}}^{\text{out}*} B_{\mathbf{p}}^{\text{in}*}] \\ & \left. \left. + \tilde{\mathcal{A}}_3 \times \int_{-\infty}^{+\infty} dx^0 e^{+ikx^0} [A_{\mathbf{p}}^{\text{out}*} B_{\mathbf{p}}^{\text{in}*} + B_{\mathbf{p}}^{\text{out}*} A_{\mathbf{p}}^{\text{in}*}] \right\} \right|^2 \\ & + \left| -ie \int_{-\infty}^{+\infty} \frac{dk}{2\pi} \left\{ \frac{m}{\sqrt{m^2 + \mathbf{p}_{\perp}^2}} (\tilde{\mathcal{A}}_1 - i\sigma \tilde{\mathcal{A}}_2) \times \int_{-\infty}^{+\infty} dx^0 e^{+ikx^0} [A_{\mathbf{p}}^{\text{out}*} A_{\mathbf{p}}^{\text{in}*} + B_{\mathbf{p}}^{\text{out}*} B_{\mathbf{p}}^{\text{in}*}] \right\} \right|^2 \Big], \quad (\text{A5}) \end{aligned}$$

where $\sigma = +1$ for $s = \uparrow$ and -1 for $s = \downarrow$ and $\tilde{\mathcal{A}}_{\mu}$ represents the Fourier transformation of \mathcal{A}_{μ} ,

$$\tilde{\mathcal{A}}_{\mu}(k) \equiv \int_{-\infty}^{+\infty} dx^0 e^{-ikx^0} \mathcal{A}_{\mu}(x^0). \quad (\text{A6})$$

By using Eqs. (A2a) and (A2b), one can rewrite the x^0 -integrations in Eq. (A5) as

$$\int_{-\infty}^{+\infty} dx^0 e^{+ikx^0} A_{\mathbf{p}}^{\text{out}*} A_{\mathbf{p}}^{\text{in}*} = e^{+i\pi/4} e^{-\pi a_{\mathbf{p}}/2} \sqrt{a_{\mathbf{p}}} \times I_{a_{\mathbf{p}}-i, a_{\mathbf{p}}}, \quad (\text{A7a})$$

$$\int_{-\infty}^{+\infty} dx^0 e^{+ikx^0} A_{\mathbf{p}}^{\text{out}*} B_{\mathbf{p}}^{\text{in}*} = e^{-\pi a_{\mathbf{p}}/2} \times I_{a_{\mathbf{p}}, a_{\mathbf{p}}}, \quad (\text{A7b})$$

$$\int_{-\infty}^{+\infty} dx^0 e^{+ikx^0} B_{\mathbf{p}}^{\text{out}*} A_{\mathbf{p}}^{\text{in}*} = e^{-\pi a_{\mathbf{p}}/2} a_{\mathbf{p}} \times I_{a_{\mathbf{p}}-i, a_{\mathbf{p}}-i}, \quad (\text{A7c})$$

$$\int_{-\infty}^{+\infty} dx^0 e^{+ikx^0} B_{\mathbf{p}}^{\text{out}*} B_{\mathbf{p}}^{\text{in}*} = e^{-i\pi/4} e^{-\pi a_{\mathbf{p}}/2} \sqrt{a_{\mathbf{p}}} \times I_{a_{\mathbf{p}}, a_{\mathbf{p}}-i}, \quad (\text{A7d})$$

where

$$I_{\lambda, \lambda'} \equiv \int_{-\infty}^{+\infty} dx^0 e^{+ikx^0} D_{-i\lambda} \left(-e^{+i\pi/4} \xi_{\mathbf{p}} \right) \left[D_{-i\lambda'} \left(e^{+i\pi/4} \xi_{\mathbf{p}} \right) \right]^*. \quad (\text{A8})$$

Noting that the parabolic cylinder function D_{ν} has the following integral expression [50]

$$D_{\nu}(\pm e^{i\pi/4} \xi) = \frac{e^{-i\xi^2/4}}{e^{i\pi\nu} \Gamma(-\nu)} \int_0^{\infty} dy y^{-\nu-1} e^{\mp i\xi y - iy^2/2}, \quad (\text{A9})$$

one can evaluate $I_{\lambda,\lambda'}$ analytically as

$$I_{\lambda,\lambda'} = \pi \sqrt{\frac{2}{e\bar{E}}} e^{-\pi(\lambda+\lambda')/4} \Theta(-k) \left(\frac{-k}{\sqrt{2e\bar{E}}} \right)^{i(\lambda-\lambda')-1} \exp \left[-i \left(\frac{k^2}{4e\bar{E}} + \frac{kp_3}{e\bar{E}} \right) \right] {}_1\tilde{F}_1 \left(-i\lambda'; -i(\lambda' - \lambda); i \frac{k^2}{2e\bar{E}} \right), \quad (\text{A10})$$

where ${}_1\tilde{F}_1(a; b; z) \equiv {}_1F_1(a; b; z)/\Gamma(b)$ is the regularized hypergeometric function and Θ is the step function. By substituting Eq. (A10) into Eqs. (A7a)-(A7d) and simplifying Eq. (A5), one obtains

$$\begin{aligned} n_{\pm\mathbf{p},s}^{(\mp)} = & \frac{V}{(2\pi)^3} e^{-2\pi a_{\mathbf{p}}} \left[\left| 1 - e \int_0^\infty dk e^{-i \frac{kp_3}{e\bar{E}}} \left\{ \frac{p_1 \tilde{\mathcal{A}}_1 + p_2 \tilde{\mathcal{A}}_2}{e\bar{E}} \operatorname{Re} \left[e^{-i \frac{k^2}{4e\bar{E}}} {}_1\tilde{F}_1 \left(1 - ia_{\mathbf{p}}; 1; i \frac{k^2}{2e\bar{E}} \right) \right] \right. \right. \right. \\ & - \sigma \frac{-p_2 \tilde{\mathcal{A}}_1 + p_1 \tilde{\mathcal{A}}_2}{e\bar{E}} \operatorname{Im} \left[e^{-i \frac{k^2}{4e\bar{E}}} {}_1\tilde{F}_1 \left(1 - ia_{\mathbf{p}}; 1; i \frac{k^2}{2e\bar{E}} \right) \right] \\ & \left. \left. \left. - i \frac{k \tilde{\mathcal{A}}_3}{e\bar{E}} a_{\mathbf{p}} \operatorname{Re} \left[e^{-i \frac{k^2}{4e\bar{E}}} {}_1\tilde{F}_1 \left(1 - ia_{\mathbf{p}}; 2; i \frac{k^2}{2e\bar{E}} \right) \right] \right\} \right|^2 \right. \\ & \left. + \left| e \int_0^\infty dk e^{-i \frac{kp_3}{e\bar{E}}} \frac{m}{\sqrt{e\bar{E}}} \frac{\tilde{\mathcal{A}}_1 + i\sigma \tilde{\mathcal{A}}_2}{\sqrt{e\bar{E}}} \operatorname{Im} \left[e^{-i \frac{k^2}{4e\bar{E}}} {}_1\tilde{F}_1 \left(1 - ia_{\mathbf{p}}; 1; i \frac{k^2}{2e\bar{E}} \right) \right] \right|^2 \right]. \quad (\text{A11}) \end{aligned}$$

For the monochromatic perturbation (5), $\tilde{\mathcal{A}}_\mu$ reads

$$\tilde{\mathcal{A}}_\mu = -i\pi \left[e^{+i\phi} \delta(k - \Omega) - e^{-i\phi} \delta(k + \Omega) \right] \times (0, a_1, a_2, a_3). \quad (\text{A12})$$

Therefore, we finally arrive at

$$\begin{aligned} n_{\pm\mathbf{p},s}^{(\mp)} = & \frac{V}{(2\pi)^3} e^{-2\pi a_{\mathbf{p}}} \left[\left| 1 + e \times i\pi e^{+i\phi} e^{-i \frac{\Omega p_3}{e\bar{E}}} \left\{ \frac{p_1 a_1 + p_2 a_2}{e\bar{E}} \operatorname{Re} \left[e^{-i \frac{\Omega^2}{4e\bar{E}}} {}_1\tilde{F}_1 \left(1 - ia_{\mathbf{p}}; 1; i \frac{\Omega^2}{2e\bar{E}} \right) \right] \right. \right. \right. \\ & - \sigma \frac{-p_2 a_1 + p_1 a_2}{e\bar{E}} \operatorname{Im} \left[e^{-i \frac{\Omega^2}{4e\bar{E}}} {}_1\tilde{F}_1 \left(1 - ia_{\mathbf{p}}; 1; i \frac{\Omega^2}{2e\bar{E}} \right) \right] \\ & \left. \left. \left. - ia_3 \frac{\Omega}{e\bar{E}} a_{\mathbf{p}} \operatorname{Re} \left[e^{-i \frac{\Omega^2}{4e\bar{E}}} {}_1\tilde{F}_1 \left(1 - ia_{\mathbf{p}}; 2; i \frac{\Omega^2}{2e\bar{E}} \right) \right] \right\} \right|^2 \right. \\ & \left. + e^2 \times \pi^2 \frac{m^2}{e\bar{E}} \frac{|a_1|^2 + |a_2|^2}{e\bar{E}} \left| \operatorname{Im} \left[e^{-i \frac{\Omega^2}{4e\bar{E}}} {}_1\tilde{F}_1 \left(1 - ia_{\mathbf{p}}; 1; i \frac{\Omega^2}{2e\bar{E}} \right) \right] \right|^2 \right]. \quad (\text{A13}) \end{aligned}$$

-
- [1] F. Sauter, “*Ueber das Verhalten eines Elektrons im homogenen elektrischen Feld nach der relativistischen Theorie Diracs*,” Z. Phys. **69**, 742 (1931).
[2] W. Heisenberg and H. Euler, “*Folgerungen aus der Diracschen Theorie des Positrons*,” Z. Phys. **98**, 714 (1936).
[3] J. Schwinger, “*On Gauge Invariance and Vacuum Polarization*,” Phys. Rev. **82**, 664 (1951).
[4] L. Landau, “*Zur Theorie der Energieübertragung. II*,” Phys. Z. Sowjetunion **2**, 46 (1932).
[5] C. Zener, “*Non-Adiabatic Crossing of Energy Levels*,” Proc. Roy. Soc. London Ser. A **137**, 696 (1932).
[6] E. C. G. Stueckelberg, “*Theorie der unelastischen Stosse zwischen Atomen*,” Helv. Phys. Acta. **5**, 369 (1932).
[7] E. Majorana, “*Atomi orientati in campo magnetico variabile*,” Nuovo Cim. **9**, 43 (1932).
[8] V. Yanovsky *et al.*, “*Ultra-high intensity 300 TW laser at 0.1 Hz repetition rate*,” Optics Express **16**, 2109 (2008).
[9] www.eli-beams.eu
[10] www.hiper-laser.org
[11] R. Schutzhold, H. Gies, and G. Dunne, “*Dynamically Assisted Schwinger Mechanism*,” Phys. Rev. Lett. **101**, 130404 (2008).
[12] A. Di Piazza, E. Lotstedt, A. I. Milstein, and C. H. Keitel, “*Barrier control in tunneling e^+e^- photoproduction*,” Phys. Rev. Lett. **103**, 170403 (2009).
[13] G. V. Dunne, H. Gies, and R. Schutzhold, “*Catalysis of Schwinger Vacuum Pair Production*,” Phys. Rev. D **80**, 111301 (2009).

- [14] A. Monin, and M. B. Voloshin, “*Photon-stimulated production of electron-positron pairs in electric field,*” Phys. Rev. D **81**, 025001 (2010).
- [15] A. Monin, and M. B. Voloshin, “*Semiclassical Calculation of Photon-Stimulated Schwinger Pair Creation,*” Phys. Rev. D **81**, 085014 (2010).
- [16] V. W. Franz, “*Einfluss eines elektrischen Feldes auf eine optische Absorptionskante,*” Z. Naturforsch. Teil A **13**, 484 (1958).
- [17] L. V. Keldysh, “*The Effect of a Strong Electric Field on the Optical Properties of Insulating Crystals ,*” Sov. Phys. JETP **7**, 788 (1958).
- [18] K. Tharmalingam, “*Optical Absorption in the Presence of a Uniform Field,*” Phys. Rev. **130**, 2204 (1963).
- [19] J. Callaway, “*Optical Absorption in an Electric Field,*” Phys. Rev. **130**, 549 (1963).
- [20] H. Taya, “*Franz-Keldysh effect in strong-field QED,*” arXiv:1812.03630.
- [21] G. Torgrimsson, C. Schneider, and R. Schutzhold, “*Dynamically assisted Sauter-Schwinger effect - non-perturbative versus perturbative aspects ,*” JHEP **06**, 043 (2017).
- [22] G. Torgrimsson, “*Perturbative methods for assisted non-perturbative pair production,*” arXiv:1812.04607.
- [23] W. H. Furry, “*On Bound State and Scattering in Positron Theory,*” Phys. Rev. **81**, 115 (1951).
- [24] E. S. Fradkin, and D. M. Gitman, “*Furry Picture for Quantum Electrodynamics With Pair Creating External Field ,*” Fortschr. Phys. **29**, 381 (1981).
- [25] E. S. Fradkin, D. M. Gitman, and S. M. Shvartsman, “*Quantum Electrodynamics with Unstable Vacuum,*” Springer-Verlag, Berlin (1991).
- [26] C. Kohlfurst, “*Spin-states in multiphoton pair production for circularly polarized light,*” arXiv:1812.03130 [hep-ph].
- [27] E. Brezin and C. Itzykson, “*Pair Production in Vacuum by an Alternating Field,*” Phys. Rev. D **2**, 1191 (1970).
- [28] V. S. Popov, “*Pair production in a variable external field (quasiclassical approximation),*” JETP **34**, 709 (1972).
- [29] L. V. Keldysh, “*Ionization in the field of a strong electromagnetic wave,*” JETP **20**, 1307 (1965).
- [30] H. Taya, H. Fujii, and K. Itakura, “*Finite pulse effects on e^+e^- pair creation from strong electric fields,*” Phys. Rev. D **90**, 014039 (2014).
- [31] G. Torgrimsson, C. Schneider, and R. Schutzhold, “*Sauter-Schwinger pair creation dynamically assisted by a plane wave,*” Phys. Rev. D **97**, 096004 (2018).
- [32] C. Itzykson, J.-B. Zuber, “*Quantum Field Theory,*” McGraw-Hill (1980).
- [33] A. I. Nikishov, “*Pair Production by a Constant External Field,*” JETP **30**, 660 (1970).
- [34] N. Tanji, “*Dynamical view of pair creation in uniform electric and magnetic fields,*” Ann. Phys. **324**, 1691 (2009).
- [35] F. Gelis, and N. Tanji, “*Schwinger mechanism revisited,*” Prog. Part. Nucl. Phys. **87**, 1 (2016).
- [36] H. Taya, “*Quark and Gluon Production from a Boost-invariantly Expanding Color Electric Field ,*” Phys. Rev. D **96**, 014033 (2017).
- [37] N. D. Birrell and P. C. W. Davies, “*Quantum Fields in Curved Space,*” Cambridge University Press (1982).
- [38] A. Di Piazza, C. Muller, K. Z. Hatsagortsyan, and C. H. Keitel, “*Extremely high-intensity laser interactions with fundamental quantum systems,*” Rev. Mod. Phys. **84**, 1177 (2012).
- [39] C. Kohlfurst, M. Mitter, G. von Winckel, F. Hebenstreit, and R. Alkofer “*Optimizing the pulse shape for Schwinger pair production,*” Phys. Rev. D **88**, 045028 (2013).
- [40] F. Hebenstreit, and F. Fillion-Gourdeau, “*Optimization of Schwinger pair production in colliding laser pulses,*” Phys. Lett. B **739**, 189 (2014).
- [41] M. F. Linder, C. Schneider, J. Sicking, N. Szpak, and R. Schutzhold, “*Pulse shape dependence in the dynamically assisted Sauter-Schwinger effect,*” Phys. Rev. D **92**, 085009 (2015).
- [42] F. E. Low, “*Model of the bare Pomeron,*” Phys. Rev. D **12**, 163 (1975).
- [43] S. Nussinov, “*Colored-Quark Version of Some Hadronic Puzzles,*” Phys. Rev. Lett. **34**, 1286 (1975).
- [44] A. Kovner, L. McLerran, and H. Weigert, “*Gluon Production at High Transverse Momentum in the McLerran-Venugopalan Model of Nuclear Structure Functions,*” Phys. Rev. D **52**, 3809 (1995).
- [45] A. Kovner, L. McLerran, and H. Weigert, “*Gluon Production from Non-Abelian Weizsäcker-Williams Fields in Nucleus-Nucleus Collisions,*” Phys. Rev. D **52**, 6231 (1995).
- [46] T. Lappi and L. McLerran, “*Some Features of the Glasma,*” Nucl. Phys. A **772**, 200 (2006).
- [47] N. K. Glendenning, and T. Matsui, “*Creation of $q\bar{q}$ pairs in a chromoelectric flux tube,*” Phys. Rev. D **28**, 2890 (1983).
- [48] K. Kajantie and T. Matsui, “*Decay of strong color electric field and thermalization in ultra-relativistic nucleus-nucleus collisions,*” Phys. Lett. B **164**, 373 (1985).
- [49] G. Gatoff, A. K. Kerman, and T. Matsui, “*Flux-tube model for ultrarelativistic heavy-ion collisions: Electrohydrodynamics of a quark-gluon plasma,*” Phys. Rev. D **36**, 114 (1987).
- [50] I. S. Gradshteyn, and I. M. Ryzhik, “*Table of Integrals, Series, and Products,*” 8th edition, Academic Press (2015).
- [51] F. Becattini and Iu. Karpenko, “*Collective Longitudinal Polarization in Relativistic Heavy-Ion Collisions at Very High Energy,*” Phys. Rev. Lett. **120**, 012302 (2018).
- [52] T. Niida (for STAR Collaboration), “*Global and local polarization of hyperons in Au+Au collisions at 200 GeV from STAR,*” Nucl. Phys. A **982**, 511 (2019).
- [53] W. -T. Deng and X. -G. Huang, “*Electric fields and chiral magnetic effect in Cu+Au collisions,*” Phys. Lett. B **742**, 296 (2015).
- [54] Y. Hirono, M. Hongo, and T. Hirano, “*Estimation of the electric conductivity of the quark gluon plasma via asymmetric heavy-ion collisions,*” Phys. Rev. C **90**, 021903 (2014).